ELSEVIER

Deep-Sea Research II 51 (2004) 1187–1203

DEEP-SEA RESEARCH
PART II

www.elsevier.com/locate/dsr2

On the seasonal correlation of surface particle fields with wind stress and Mississippi discharge in the northern Gulf of Mexico

Joseph E. Salisbury[a,e,*], Janet W. Campbell[a,f], Ernst Linder[b], L. David Meeker[c], Frank E. Müller-Karger[d], Charles J. Vörösmarty[e,f]

[a]*Ocean Process Analysis Laboratory Institute for the Study of Earth, Oceans, and Space University of New Hampshire, Durham, NH, USA*
[b]*Department of Mathematics and Statistics, University of New Hampshire, Durham, NH, USA*
[c]*Climate Change Research Center Institute for the Study of Earth, Oceans and Space, University of NH, Durham, NH, USA*
[d]*College of Marine Science, University of South Florida, St. Petersburg, FL, USA*
[e]*Water Systems Analysis Group, Complex Systems Research Center, Institute for the Study of Earth, Oceans, and Space, University of New Hampshire, Durham, USA*
[f]*Department of Earth Sciences, University of New Hampshire, Durham, NH, USA*

Received 2 August 2002; accepted 15 March 2004
Available online 25 August 2004

Abstract

Spatio-temporal correlation analyses were performed on time series of daily freshwater discharge, wind fields, and SeaWiFS-derived surface particle concentrations in the northern Gulf of Mexico. The influences of discharge and winds on surface particle concentrations were investigated by mapping temporal correlation coefficients at each pixel for the whole time series (1997–2000) and for each season during 1999 and 2000. Maps of the correlation between suspended particulate matter concentration (SPM) and river discharge suggest regions that are fluvially influenced. The particulate matter may be sediments carried by the river plume or biogenic particles (e.g., detritus) stimulated by the river discharge. The algorithm used to estimate SPM concentrations does not differentiate between sediment and detritus. Maps of the correlation between wind stress and SPM suggest regions where wind mixing accounts for particulate resuspension and subsequent transport. Regions of significant positive wind-SPM correlation were independent, and often spatially separated, from regions of strong positive discharge-SPM correlation. Thus, the influences of winds and discharge on particle distributions can be investigated independently.

Regions of high wind-SPM correlation were associated with shallow shelf areas, as correlation contours generally followed the bathymetric contours, and expanded in size under offshore wind regimes. These areas exhibited less spatial and temporal variability than the regions of high discharge-SPM correlation associated with the Mississippi-Atchafalaya river system. There was no apparent relationship between the magnitude of Mississippi- Atchafalaya discharge and the spatial extent of the region of high discharge-SPM correlation during seasonal analyses. Instead, the

*Corresponding author. Ocean Process Analysis Laboratory Institute for the Study of Earth, Oceans, and Space University of New Hampshire, Durham, NH, USA. Tel.: +1-603-862-0849.
E-mail address: joe.salisbury@unh.edu (J.E. Salisbury).

0967-0645/$ - see front matter
doi:10.1016/j.dsr2.2004.03.002

spatial extent and orientation of the discharge-SPM correlation field appeared to be a function of winds (both their direction and speed) and the buoyancy of the plume.

1. Introduction

Knowledge of the source, transport and fate of suspended sediment in the coastal ocean is of critical importance because of the co-occurrence of sediment with pollutants, nutrients and carbon constituents. Large rivers, the major conduits linking terrestrial and coastal marine environments, are integral systems in the delivery and cycling of minerogenic and bioactive constituents. The role of river-borne sediments as carriers of organic and elemental pollutants from the land to the coast has been described in detail (Meybeck, 1982; Long, 2000; Villaescusa-Celaya et al., 2000). Suspended sediment alters light availability in the water column, and thus is an important factor regulating the spatial and temporal patterns of coastal productivity (Chen et al., 2000; Lohrenz et al., 1999; Demaster et al., 1996; Cloern, 1987). Coastal sediment plume regimes are sites of intense downward particle flux, and riverine-delivered sediments are a substrate for vigorous biogeochemical activity (McKee et al., 2004; Amon and Benner, 1996). The transformation and fate of riverine particulate (and dissolved) carbon constituents in coastal waters play an important role in global carbon cycling. In light of global and regional issues arising from the interaction of land-derived particulate constituents in coastal waters, a better understanding of the spatial and temporal dynamics of SPM in coastal waters is needed.

To study the presence and transport of constituents in coastal waters requires the ability to make measurements over large spatial domains at relatively high spatial and temporal resolution. This requirement coupled with financial considerations limits the use of in situ shipboard measurements in studies covering vast coastal domains. Satellite remote sensing provides the only reasonable means of obtaining the synoptic data required for such a study. Several investigators have used satellite data in the study of the source, trajectory and fate of riverine plumes. These investigators have used a variety of sensors including Landsat (Rouse and Coleman, 1976; Stumpf, 1988), the Coastal Zone Color Scanner (CZCS) (Müller-Karger et al., 1989; Müller-Karger et al., 1991; Tassan and Sturm, 1986), the Advanced Very High Resolution Radiometer (AVHRR) (Siegel and Gerth, 2000; Walker, 1996; Walker et al., 1994; Stumpf and Goldschmidt, 1992; Stumpf and Pennock, 1989), the Sea-viewing Wide Field-of-view Sensor (SeaWiFS) (Mertes and Warrick, 2001; Siddorn et al., 2001; Salisbury et al., 2001; Myint and Walker, 2002), and the Moderate-resolution Imaging Spectroradiameter (MODIS), (Moeller et al., 2001).

To investigate the correlation of wind and discharge with SPM, we have used time series of SeaWiFS data, gridded wind products from the National Centers for Environmental Prediction (NCEP), hourly buoy data from the National Buoy Data Center (NBDC), and daily discharge data from the United States Geological Survey (USGS) and United States Army Corps of Engineers (USACE). We hypothesize that certain time-varying land-based processes (e.g., terrestrial fluxes to the coast) covary predictably with ocean-color fields proximal to river discharge points. Furthermore, we believe it possible to gain understanding of the presence, transformation and fate of riverine constituents through knowledge of the spatio-temporal distribution of the ocean-color field.

In this study, we demonstrate these concepts in the northern Gulf of Mexico. Within three-month seasons in 1999 and 2000, we determine and map the correlation between (a) the Mississippi's discharge and SeaWiFS-derived SPM, and (b) NCEP-derived local wind stress and the SeaWiFS-derived SPM. We then investigate the role of wind stress and wind direction on the position and extent of the Mississippi's influence as inferred by the correlation fields.

2. Background

The northern Gulf of Mexico contains biophysical systems of considerable regional and global significance. This is particularly true of the vast area of the Gulf influenced by North America's largest river, the Mississippi. This region is highly productive in terms of phytoplankton (Hitchcock et al., 1997) and zooplankton (Ortner et al., 1989) abundance and contributes over a quarter of the total fisheries production (in dollar value) in the United States (NSF, 2002). Productivity in the region is enhanced by the Mississippi's nutrient enrichment, which has been substantially impacted by anthropogenic activity over its extensive drainage basin in recent years. Indeed, it is estimated that in the last 40 years, inorganic nitrogen fluxes to the Gulf have doubled (Goolsby and Battaglin, 2001; Rabalais et al., 1996) and silicate fluxes have decreased (Turner et al., 1998; Justic et al., 1995) as a result of this activity. Excessive productivity has led to deleterious consequences such as the well-publicized seasonal hypoxic events that occur west of the Mississippi Delta (Justic et al., 2002).

In terms of climatological discharge, the Mississippi is the largest North American river and the 6th largest river in the world (Fekete et al., 1999). It drains over 40% of the contiguous United States, with much of its basin involved in agricultural activity (Goolsby and Battaglin, 2001). The Mississippi River is the dominant source of sediment to the northern Gulf of Mexico. Based on data from 1963 to 1979 the Mississippi/Atchafalaya System had an average suspended sediment delivery of approximately $210 \times 10^9\,\mathrm{kg\,y^{-1}}$ (Milliman and Meade, 1983). Although this figure is widely quoted, at present the annual flux is thought to be less due to sediment retention in recently built reservoirs and improved agricultural practices (M. Meybeck, personal communication, 2002). For example, during the period of study, January 1, 1999–December 31, 2000, the Mississippi delivered approximately $91.2 \times 10^9\,\mathrm{kg\,y^{-1}}$ of suspended sediment of which $\sim 1.4 \times 10^9\,\mathrm{kg\,y^{-1}}$ was particulate organic matter (NASQAN, 2001).

The area of study is the northern Gulf of Mexico (Fig. 1). Although there are several rivers that contribute substantial discharge to the study area (e.g., Appalachicola, Alabama/Tombigbee), the Mississippi typically accounts for over 60% of the total discharge (Fekete et al., 1999). Freshwater from the Mississippi has been reported to extend over 1000 km to the west (Dinnel and Wiseman, 1986). It also has been observed 700 km to the southeast, exiting the Gulf through the Florida Straits and thus occasionally entering the western Atlantic. A contiguous salinity signal from the Mississippi was mapped around the Florida Keys and as far north as Georgia (Atkinson and Wallace, 1975).

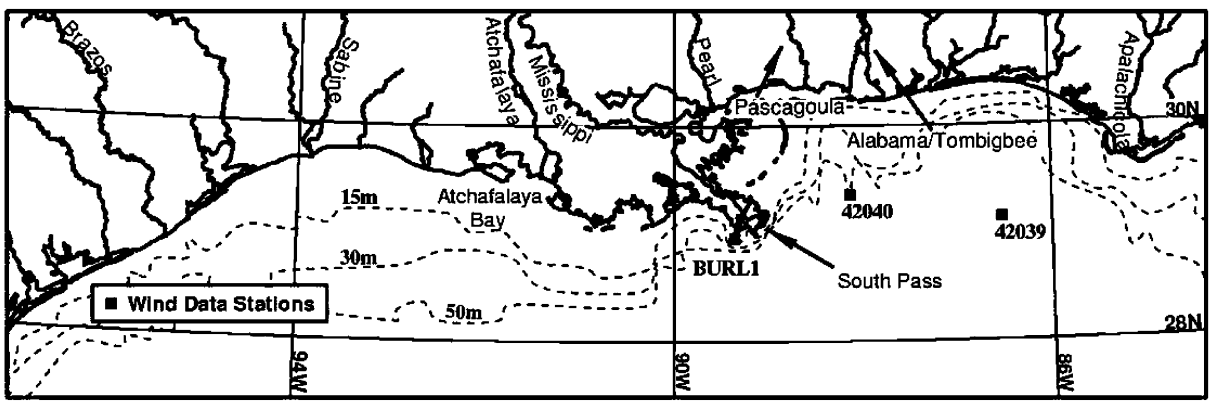

Fig. 1. Map of the northern Gulf of Mexico region with rivers and wind data station locations labeled. Isobaths of 15, 30 and 50 m are shown.

Water from the Mississippi enters the Gulf of Mexico through two major distributaries. The main stem of the Mississippi carries ~70% of the discharge through a bird's foot delta and enters the Gulf in deep water beyond the shelf break. The Atchafalaya, which has been engineered to carry the remaining ~30% of the discharge, exits onto a broad inner shelf environment with water depths of only ~5 m. The diurnal tidal range, which is small (~20–40 cm), typically generates surface currents less than 15 cm s^{-1} (Murray, 1972; Adams et al., 1982). Tidal components were shown to have a minimal effect on Mississippi plume morphology (Walker, 1996), and probably do not play a major role in sediment resuspension and transport processes (see Booth et al., 2000). In shallow shelf environments such as the vicinity of the Atchafalaya discharge and the Louisiana-Texas Shelf, intermittent wind-induced mixing and wave-induced resuspension of sediment is common (Allison et al., 2000; Walker and Hammack, 2000; Drake and Cacchione, 1986). Intense wind events associated with the passing of low-pressure systems on 3–7 day time scales (from October to April) are thought to be the dominant mechanism for sediment transport to deeper waters in this region (Allison et al., 2000).

The orientation of freshwater proximal to the Mississippi's discharge points is primarily regulated by wind and subsequent current patterns. Although winds in the northern Gulf of Mexico exhibit no distinct seasonal cycle (Gutierrez de Velasco and Winant, 1996), a bimodal wind regime is common during most years. Cochrane and Kelly (1986) illustrated that persistent easterly winds over the northern Gulf tend to set up a westward flow over the shelf throughout much of the year. The results of this westward flow are apparent in surface salinity surveys that show the presence of Mississippi water well to the west of its source during much of the year (Dinnel and Wiseman, 1986; Sahl et al., 1997; Li et al., 1997). During the summer, however, westward flow is often interrupted by periods of southerly to westerly winds that induce eastward and southward flow regimes. The westward flow is usually re-instituted in the fall with the onset of northerly to easterly winds.

In addition to bimodal flow brought on by seasonal wind variability, flow near the shelf edge is modified by the Coriolis effect as well as eddies and filaments shed by the Loop Current. Several authors have described enhanced easterly and southeasterly flow of the Mississippi's plume in the presence of anticyclonic eddies located seaward of the plume (Morey et al., 2003; DelCastillo et al., 2001; Müller-Karger, 2000). Surface imagery of the sediment plume often reveals a small anticyclonic feature close to the discharge point at South Pass (Rouse and Coleman, 1976; Salisbury et al., 2001; Walker, 1996). Although this could be explained by the Earth's rotation, the Mississippi plume has a Kelvin number less than 1 (Garvine, 1995), and thus the Coriolis acceleration plays a smaller role in the development of plume morphology compared to the combined effects of winds and currents.

3. Data and methods

3.1. Ocean color satellite data

Level-2 SeaWiFS data were obtained from the NASA Goddard Distributed Active Archive Center (Goddard-DAAC). These data (known as global area coverage, or GAC data) comprise 1-km pixels subsampled at 4-km resolution. They had been processed with the SeaDAS version 4.0 software (Baith et al., 2001) using the atmospheric correction algorithm of Siegel et al. (2000), and the OC4v4 chlorophyll algorithm (McClain et al., 2000; O'Reilly et al., 2000). The resultant chlorophyll (CHL) and normalized water-leaving radiances (nLw) in the first 6 bands were then mapped to the projection shown in Fig. 1, and passed through a 3×3 median filter to remove speckling in band 6 (670 nm). Daily images of CHL and nLw were produced for all available days from 9/20/97 (the beginning of the SeaWiFS mission) to 12/31/00.

A simple single-band algorithm based on the water leaving radiance at 670 nm (SeaWiFS band 6) was then used to estimate SPM at each pixel. Reflectance of light at this wavelength tends to be enhanced in the presence of suspended sediments

(Kirk, 1994; Whitlock et al., 1981), whereas it is least affected by the biological and photochemical variability found in optically complex coastal waters (IOCCG, 2000). In earlier work, we used the 670-nm radiance as an index of sediment concentration, but the relationship between nLw(670) and sediment concentration is nonlinear at high concentrations. In this work, we sought an algorithm in which particle concentration varied monotonically with nLw(670), and which gave realistic SPM concentrations as compared with earlier published results (Walker, 1996, Stumpf et al., 1993).

The SPM algorithm we used was based on an algorithm of Walker (1996) that was developed for atmospherically corrected AVHRR data and parameterized for the Mississippi River plume. The algorithm is intended to retrieve total suspended particulates, which includes minerogenic sediments as well as phytoplankton detritus and other detritus of organic origin.

The algorithm of Walker was based on the semi-analytic model of irradiance reflectance described by Stumpf and Pennock (1989). According to this model, irradiance reflectance in a moderately turbid estuary is dominated by the backscattering of sediment. It is modeled as

$$R = \frac{yF}{1 + G/n}, \tag{1}$$

where n is the suspended sediment concentration in $\mathrm{mg\,l^{-1}}$; y is a nonspectral constant ($y = 0.178$), and where

$$F = \frac{b^*}{a^* + b^*} \tag{2}$$

and

$$G = \frac{a_x}{a^* + b^*}. \tag{3}$$

In these equations, b^* and a^* are the specific absorption and backscattering coefficients for sediment, and a_x is the absorption coefficient for nonsediment materials including water. Solving (1) for n, we obtained the formula:

$$n = \frac{GR}{yF - R}. \tag{4}$$

Both F and G are spectrally variable, and G is a function of the concentration of chlorophyll and other constituents. However, at the red end of the spectrum, G can be considered nearly constant (Stumpf and Pennock, 1989). For these parameters, we used the values $F = 0.35$ and $G = 30.3$ proposed by Walker (1996) for the Mississippi River plume. The Walker algorithm was applied to atmospherically corrected reflectance in the AVHRR visible band (580–680 nm). We applied the same algorithm to the SeaWiFS band 6. Water-leaving radiance at 670 was converted to reflectance by dividing it by $E_d/Q \approx 153.41$, where E_d is the downwelling solar irradiance at 670 nm, and Q is the ratio of irradiance to radiance.

When applied to the SeaWiFS data, this algorithm gave reasonable results. Patterns of concentration were similar to those found in this region (Walker, 1996, Stumpf et al., 1993) and in other river-dominated coastal waters (Siegel and Gerth, 2000; Stumpf and Goldschmidt, 1992). For example, the range of SPM concentrations shown in Fig. 2 compare favorably with sediment concentrations reported by Walker (1996). In this 8-day composite map, the mean suspended particulate concentration in turbid waters less than 40 m deep was $16.7\,\mathrm{mg\,l^{-1}}$, and the median was $9.6\,\mathrm{mg\,l^{-1}}$. For all regions of significant fluvial influence (as defined below) in the SeaWiFS data analyzed in this study, the mean and median concentrations were 2.38 and $1.30\,\mathrm{mg\,l^{-1}}$, respectively.

Admittedly, this qualitative comparison with published sediment concentrations does not validate the algorithm. Any particle concentration algorithm should be carefully validated with in situ measurements before it is used for quantitative assessments of particle concentration. For the correlation analyses of this study, we could have simply used the 670-nm radiance as in index of suspended matter. Results might have been similar. Instead, we chose an algorithm that transformed the radiance nonlinearly in an effort to give a more realistic measure of the suspended matter concentration.

3.2. Wind data

A time series of daily NCEP winds and hourly buoy measurements of wind speed and direction

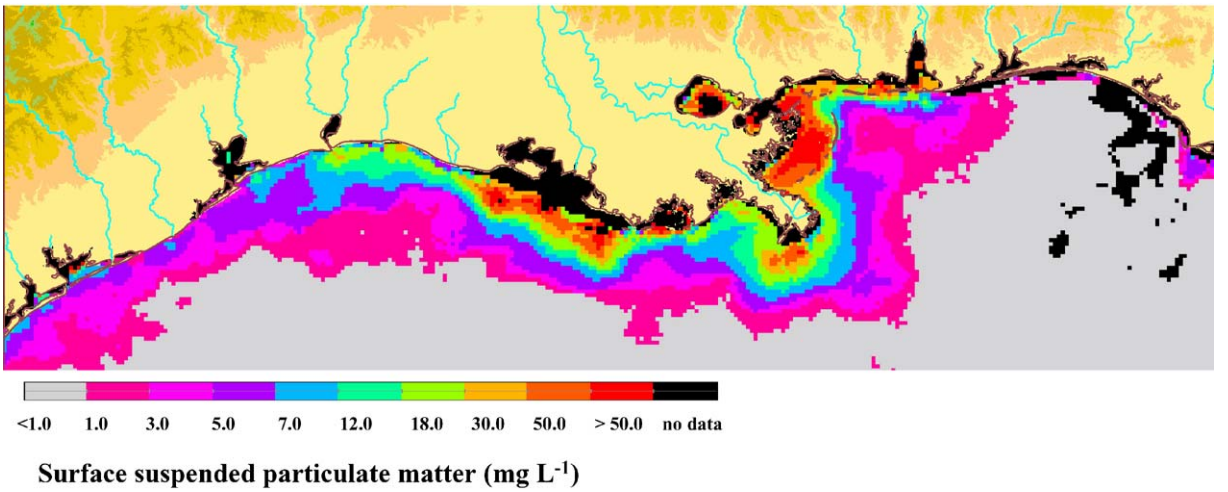

Fig. 2. Surface-suspended particulate matter distributions based on the algorithm applied to SeaWiFS data and composited over an 8-day period (4-19-99 to 4-26-99).

were used in this study. Global gridded (1°) meridional and zonal wind speed data were obtained from NCEP. These wind fields are produced four times daily (00Z, 06Z, 12Z or 18Z, where Z refers to Greenwich Mean Time). The data at 18Z were used in this study, as they are the data closest in time to the SeaWiFS satellite pass. From the wind speed components, we computed wind stress using the algorithm of Large and Pond (1981). The NCEP wind data were gridded to 4 km to correspond with the SeaWiFS data.

In addition, hourly measurements of wind speed and direction for the period 1/1/1999–12/31/2000 were obtained for three stations managed by the NDBC. These data were used to show the temporal variability of wind speeds and directions near the Mississippi's discharge points. The wind data stations (shown on Fig. 1) were identified as station BURL-1 at Southwest Pass, LA; buoy 42040, south of Dauphin, AL; and buoy 42039, south of Pensacola FL. The data stations selected provided excellent temporal coverage, reporting over 97% of all possible hourly readings. These data were pooled, temporally sorted, and hourly wind stress (Large and Pond, 1981) was calculated from the wind speed data. Histograms of wind speed and wind direction were generated for each

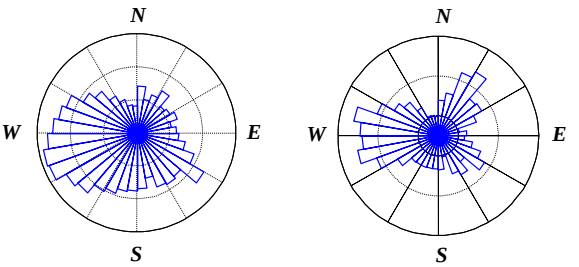

Fig. 3. Wind roses for hourly winds (left) and for stress-weighted winds (right) for the period July–September 2000, based on three buoys. Note that the stress-weighted wind rose shows a dominance of wind stress from westerly winds (blowing toward the east), and a second mode of strong northeasterly winds. The second mode is not as obvious in the simple wind rose on the left.

3-month season. Wind direction histograms are commonly reported in the form of wind roses (Fig. 3) where the wind direction is the direction from which the wind originates. Thus, for example, a *northerly wind* is blowing towards the south. For the analyses related to wind direction in this study, we weighted the wind directions by the wind stress and formed stress-weighted wind roses. In some seasons (Fig. 3) the two wind rose patterns are quite distinct. The stress-weighted wind

directions indicate the dominant directions of wind-forced momentum flux into the ocean.

3.3. Discharge data

Daily measurements of river discharge for the Mississippi River at Tarbert's Landing were obtained from the United States Army Corps of Engineers. For other large rivers emptying into the northern Gulf of Mexico, daily data for the station most proximal to the coast were obtained from the USGS. These data were used to investigate the extent to which the discharges from other rivers covary with the Mississippi discharge, thus affecting the results presented. The correlation between the Mississippi River discharge and that of other large rivers varied seasonally and interannually (Table 1), and in some seasons, discharges from the smaller rivers were negatively correlated with that of the Mississippi. The Atchafalaya was the most highly and consistently correlated with the Mississippi, as expected, and thus we consider the results to represent fluvial influence by both rivers. The years selected for analysis were variable in average annual discharge. Compared to the 1928–1986 average Mississippi discharge, 1998 was 28% above average, 1999 was 5% above average and 2000 was 29% below average.

3.4. Correlation methods

At every pixel in the satellite data, the correlation between SPM and the Mississippi discharge and between the SPM and wind stress were computed and mapped using the time series of discharge, NCEP wind stress, and SPM. Correlations were computed from 8-day averaged data over the entire time series (10/1/97–12/31/00), and from daily data for 3-month seasons in 1999 and 2000. When this was done initially without screening the data, we sometimes found regions of high correlation between discharge and SPM located far offshore. These anomalous values were the result of dividing the covariance by a small (nearly zero) standard deviation. Covariance maps (instead of correlation maps) did not exhibit this problem, but covariances were unsatisfactory because they have little physical meaning. We subsequently found that coastal regions could be distinguished from offshore areas based on a threshold value for the temporal variance of the SPM. (Others authors have simply used a threshold for the SPM, but we obtained better results by using a variance threshold.) For all analyses, we eliminated pixels in which the temporal standard deviation was less than 0.05 mg/l. For the remaining pixels, the average 90-day temporal standard deviation was 0.52 mg/l (the median was 2.68 mg/l). By masking out pixels in which the temporal variance of the sediment field was close to zero, we effectively removed the oceanic waters from the analyses.

Fig. 4 shows data time series at two locations and illustrates the degree of coherence between signals where there is a high positive correlation between discharge and SPM (Fig. 4A) and between wind and SPM (Fig. 4B). (Plot 4A corresponds to box A, Fig. 5A, and plot 4B corresponds to box B, Fig. 5B).

Table 1
Correlation values (r) between the Mississippi's discharge and the rivers indicated in the table

	January–March 99	April–June 99	July–September 99	October–December 99	All data 1998–2000
Atchafalaya	0.92	0.95	0.99	0.86	0.97
Sabine	0.24	−0.11	0.58	0.46	0.45
Brazos	0.21	0.31	0.83	0.43	0.34
Pearl	0.47	0.07	0.82	0.46	0.54
Pascagoula	0.29	0.03	0.81	0.25	0.51
Alabama/Tombig	0.25	−0.15	0.72	0.38	0.47
Appalachicola	0.54	−0.18	0.81	0.42	0.50

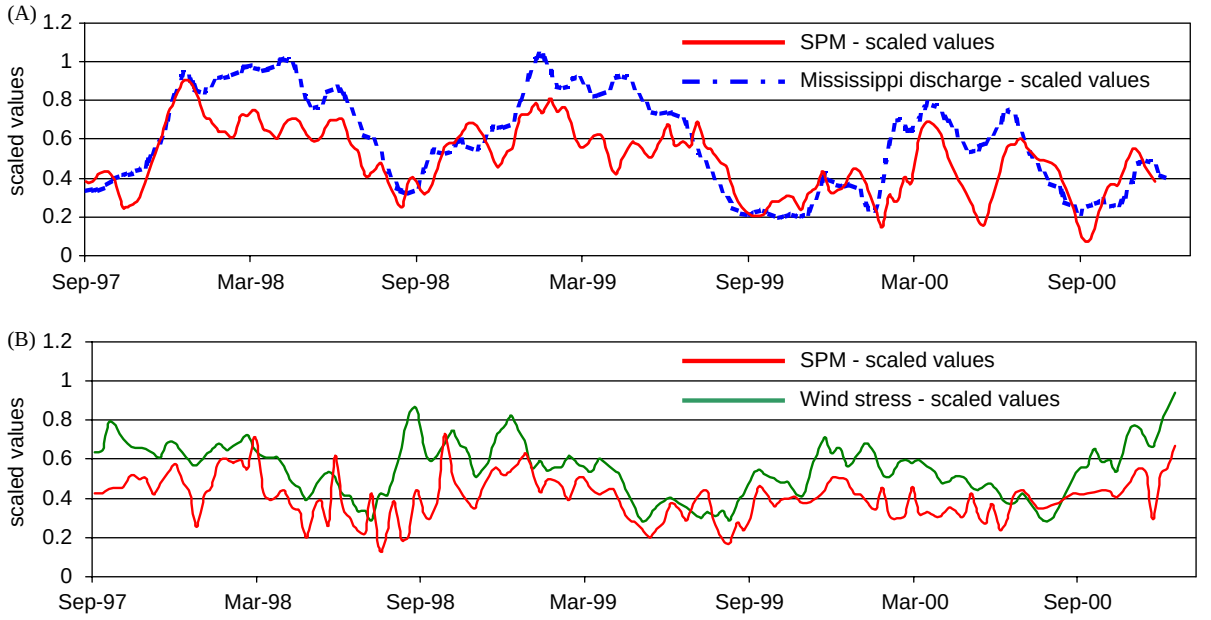

Fig. 4. Time series of the Mississippi river discharge, wind stress, and average SPM derived from SeaWiFS data for two locations: (A) a 4×4 pixel box located near the mouth of the Mississippi River (see box A in Fig. 5A) where there is a high correlation between discharge and SPM. (B) a 4×4 pixel box located in a region where there is a high correlation between wind stress and SPM (see box B in Fig. 5B).

To define regions of *significant* influence either by winds or discharge, we calculated a statistical confidence level for each pixel. The confidence level was defined as one minus the probability of obtaining that correlation from a pair of random, uncorrelated time series. Only pixels whose correlations had a statistical confidence of 95% or greater were mapped. [i.e., The hypothesis H_0: correlation = 0 was tested at each pixel, and only pixels for which this hypothesis was rejected at the $\alpha = 0.05$ level were retained.] Thus, we delineated regions *significantly influenced* by the forcing of winds or discharge.

Finally, for discharge-sediment correlations, we used an algorithm to gather only those pixels proximal to the Mississippi and Atchafalaya Rivers that were significantly correlated with the discharge. The algorithm searches out from the discharge points of the two rivers until it encounters correlated pixels and stops searching when a break in the connectivity is found. By this method, we attempted to eliminate pixels that were influenced by other rivers whose discharge co-varied with the Mississippi.

It is important to note that regions in which high or significant correlations exist between SPM and discharge (or SPM and wind stress) do not necessarily signify regions of high sediment concentration. Whenever the forcing variable is temporally in phase with SPM, significant correlations will exist regardless of the absolute concentrations. Conversely, regions of high sediment concentration did not always show significant correlations with wind or discharge. For example, the regions immediately adjacent to Atchafalaya Bay and to the west of South Pass were sometimes not included. This is a shallow (<10 m) and exceptionally turbid region where the SeaWiFS data often failed various quality tests in SeaDAS. Thus, the number of SPM determinations there tended to be low for the 3-month runs (median = 7), and the pixels often were eliminated because they failed the statistical test for significance. Alternatively, it could be that these regions

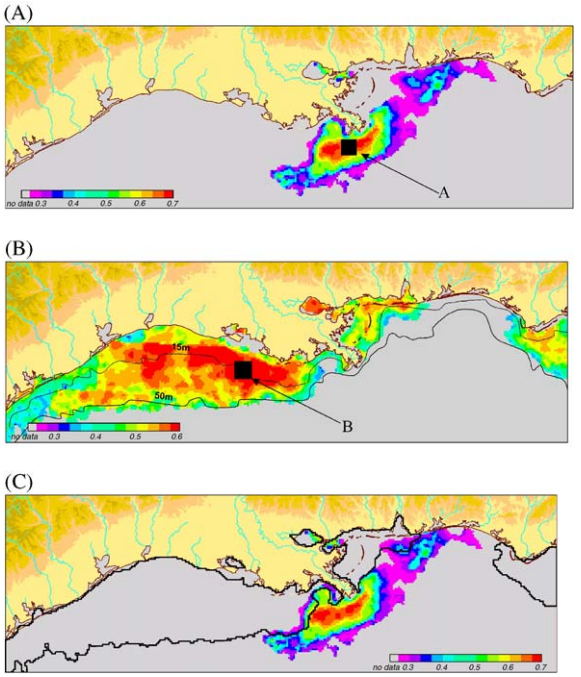

Fig. 5. Correlation maps for the period 10-01-1997 to 12-31-2000 based on 8-day average discharge, ocean color and wind speed data: (A) Region of significant correlation between the Mississippi discharge and the SPM. This region is presumed to be influenced by both the Mississippi and Atchafalaya discharges. (B) Region of significant correlation between the wind stress and the SPM. (C) Combined figure in which wind-influenced regions shown in (B) are outlined with contour lines superimposed on the map shown in (A).

were neither significantly correlated with wind stress nor discharge as a result of interference by the two temporal signals.

We assigned a significance level to the correlations based on a simple statistical hypothesis test performed at each pixel. If the null hypothesis were true (i.e., there was no correlation between the two series), one would expect that about 5% of the pixels tested would be considered significantly influenced given the choice of α, the probability of rejecting a true hypothesis, of 5%. This test allowed correlations as low as ($r = \sim 0.2$) to pass. Although these are not strong correlations, the fact that they are in a contiguous correlation field gives additional evidence that they being influenced by the discharge or wind (Linder, E., personal communication). In the case of a satellite image, one might expect somewhat more significant pixels since adjacent pixels are correlated with one another. To explore this issue, we randomly reordered (i.e., scrambled) the discharge time series and computed the sediment-discharge correlations. This was repeated 100 times for randomly selected 3-month time series. The number of significant correlations found in these runs was only about 11% of those found when the discharge series were intact. Furthermore, the significantly correlated pixels were generally not distributed in spatially coherent regions. Although this set of simulations could have been used to determine the level of significance more rigorously, we decided to use the simple method described above. The actual level of significance is not important, as long as there is a consistency in how it is defined.

A contiguous region in which the discharge is significantly positively correlated with the SPM will be referred to as a discharge-influenced region (DIR). A region of significant positive wind stress-SPM correlation will be referred to as a wind-influenced region (WIR).

4. Results

Correlation maps based on the entire time series (10/1/97–12/31/00) reveal the long-term correlation fields (Figs. 5A–C). A region of high correlation ($r > 0.7$) between the Mississippi discharge and SPM (Fig. 5A) was located near the delta and a region of significant but lower correlations extended eastward toward the Alabama coast. This region of fluvial influence was spatially separate from the regions where wind stress-SPM correlations were significant (Fig. 5B). The wind-influenced regions were associated with shallow shelf areas. The boundary of the wind-influenced region off the Louisiana-Texas coast is aligned with the 50-m isobath, and the waters with highest correlation ($r > 0.6$) had depths less than 20 m. It is unlikely that wave-generated resuspension processes could routinely affect particle dynamics beyond the 20-m isobath, and at such depths SPM concentrations were typically low. The seaward extension of the correlation field is

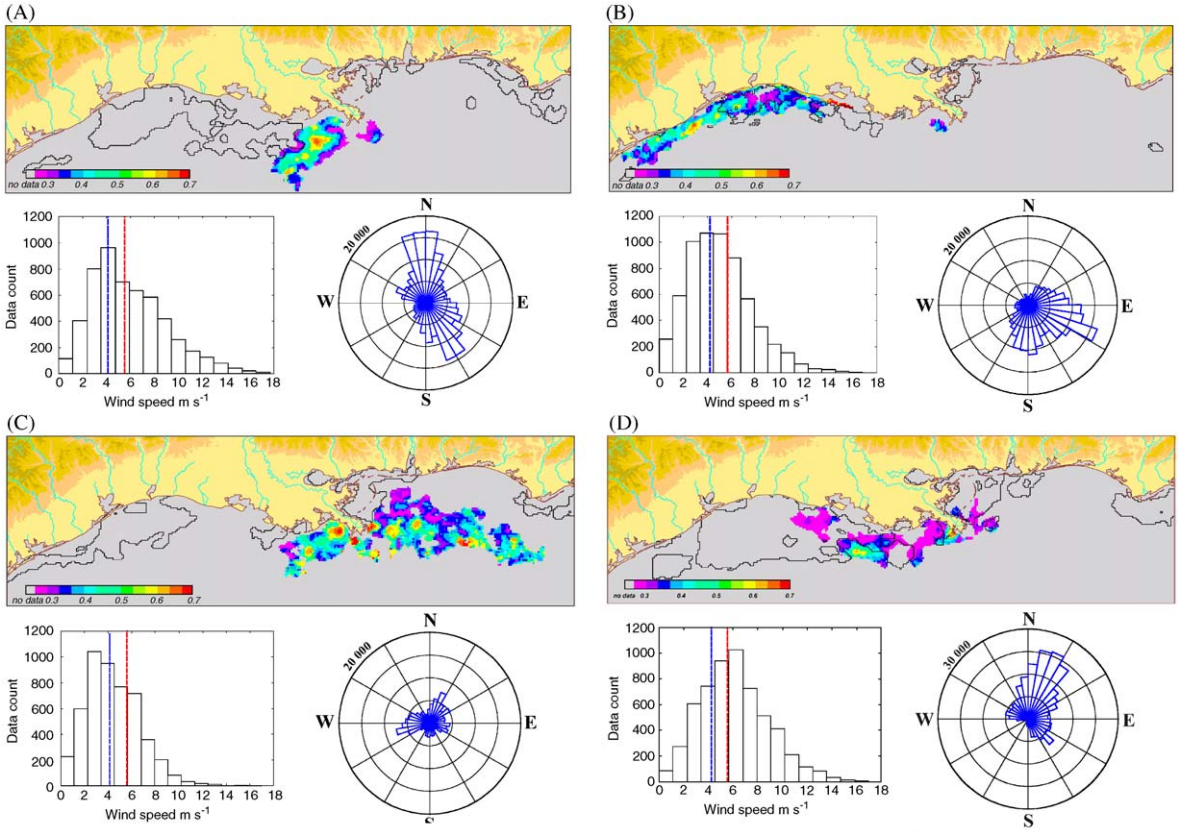

Fig. 6. Seasonal (3-month) correlation maps for 1999 based on daily data. Included for each season are histograms of the frequency distribution of wind speed and wind stress weighted directional histograms (rose diagrams). Black contours indicate the spatial extent of significant wind influence. On the wind speed histograms, the blue line shows the mode of the 3-year time series (1998–2000) and the red line shows the mean. Note the change in scale in the October–December figure: (A) January–March 1999. (B) April–June 1999, (C) July–September 1999, (D) October–December 1999.

probably related to the offshore transport of fine materials that have been suspended over the shallow areas.

In Fig. 5C, contour lines outlining the WIRs of Fig. 5B are drawn on the discharge-sediment correlation map of Fig. 5A. This format enables simultaneous viewing of the regions influenced by discharge and wind stress, and is used in the following figures. In Fig. 5C, the DIR and WIR fit together like pieces of a jigsaw puzzle, suggesting disjoint regions of dominance by the two sediment mobilization and/or transport processes (i.e., sediment delivery by rivers versus wind-driven resuspension and subsequent transport). We infer that a combination of buoyant flow, wind stress and its Ekman response are the primary determinants of the position and extent of the DIR, and that the WIR is largely an expression of wind-driven processes of resuspension and transport from shallower to deeper waters.

Seasonal correlation maps generated using daily SeaWiFS-derived sediment maps and daily discharge are shown in Figs. 6A–D. These were run over 3-month periods starting with January–March 1999 and ending with October–December 1999. Each of the correlation maps is accompanied by figures showing a histogram of wind speeds and a stress-weighted wind directional rose for the same period. As in Fig. 5C, the regions of significant WIR are indicated by black contour

Table 2
Statistics for seasonal correlation runs (1999–2000)

	Cumulative discharge ($\times 10^7$ ft^3)	Average wind speed (m s^{-1})	Mode of wind directional count multiplied by wind stress	Size of DIR (km^2)	Size of WIR (km^2)
January–March 99	7.06	5.99	Bimodal (N & SE)	1.70×10^4	2.76×10^5
April–June 99	6.30	4.93	Southeast	2.53×10^4	1.07×10^5
July–September 99	3.00	4.54	Bimodal (W & NE)	4.74×10^4	1.54×10^5
October–December 99	1.72	6.27	Northeast	2.22×10^4	4.61×10^5
January–March 00	2.85	6.08	Bimodal (NE & SE)	0.84×10^4	2.67×10^5
April–June 00	4.20	5.45	East	1.96×10^4	2.19×10^5
July–September 00	2.82	4.51	Bimodal (W & NE)	4.45×10^4	3.44×10^5
October–December 00	2.30	6.47	Northeast	4.46×10^4	5.25×10^5

lines, and correlations in the DIR are indicated by the colors. Table 2 gives the areas of the DIR and WIR for each of the seasonal correlation runs in 1999 and 2000, as well as the cumulative discharge, average wind speed, and the wind direction mode.

During the period January–March 1999 (Fig. 6A), winds were bimodal. The primary mode was from the north and the secondary mode from the southeast. The DIR was located to the southwest of the Mississippi's discharge point, and its orientation was northeast–southwest in response to the bimodal wind regime. The trajectory of the DIR can be explained by advection set up by the dominant offshore wind accompanied by Ekman transport to the right of the direction of the wind. Alternatively, the trajectory of the DIR could be the result of advection under the influence of both modes of the wind field (north and southeast). As in the other correlation runs, the WIR is confined to shallow waters, most notably the Louisiana-Texas shelf and near coastal Mississippi, Alabama and Florida.

A very different situation existed in April–June 1999 (Fig. 6B). During this period, the DIR extends westward from the Atchafalaya outfall and is positioned tightly against the Louisiana-Texas coast. Such an orientation represents the likely position of a buoyant water parcel originating from the Mississippi/Atchafalaya in the presence of a downwelling wind regime (Fong and Geyer, 2001, 2002). This pattern is thought to be caused to the combined response of advection from the westward flow driven by the alongshore component of the wind stress and Ekman dynamics moving the plume toward the coast. Particulate fluxes from the various Texas Rivers may have influenced the correlation pattern, although the covariance between these rivers and the Mississippi/Atchafalaya is generally low (Table 1).

The WIR during April–June 1999 was the smallest measured (Table 2), and like the DIR, it was positioned inside the 15 m contour along the Louisiana-Texas coast. Winds were light (4.93 m s^{-1}) during this period. We presume the narrowing of the WIR along the coast was also a response to downwelling winds. The region of the Louisiana-Texas Shelf in which the DIR and WIR overlap suggests a joint influence of wind and discharge on the correlation patterns at this location.

During the July–September 1999, time period (Fig. 6C), the DIR extended both to the east and west of the Mississippi delta, and was the largest in total area (4.74×10^4 km^2) of any season studied (Table 2). This was a period of light average winds, modest discharge, and warm sea-surface temperatures—conditions that support stratification. As suggested by Walker (1996), stratification of the water column plays an important role in the way a plume responds to wind forcing. Specifically, under highly stratified conditions where little wind mixing occurs, a buoyant plume will spread horizontally and can be easily advected in the

presence of light winds (Kudryavtsev and Soloviev, 1989). The bi-directional orientation of the DIR can be partially explained by wind advection. The plume waters were subjected to a bimodal wind regime with the primary mode coming from the west. It should be noted, however, that it is probable that an anticyclonic flow regime set up by the presence of warm core rings also influenced the flow. Sea-level anomaly maps supplied by the Naval Research Laboratory (http://www7300.nrlssc.navy.mil/altimetry) indicate the presence of a persistent positive anomaly directly south of the DIR during this time period. Velocities within such eddies can exceed $100\,cm\,s^{-1}$ and thus an eddy may have been a mechanism by which particles and dissolved materials were transported offshore (Morey et al., 2003).

For the July–September period, the area of the WIR was small ($1.54 \times 10^5\,km^2$), and likely a response to the light average winds ($4.54\,m\,s^{-1}$) recorded during this time. Nearly all of the WIR was confined to waters less than 20 m.

During October–December 1999 (Fig. 6D), the DIR originated from both the Mississippi and the Atchafalaya rivers. At this time the discharge was the lowest ($1.72 \times 10^7\,m^3\,s^{-1}$), and the average wind speed was high ($6.27\,m\,s^{-1}$). The winds were from the northeast and a combination of advection and Ekman transport could explain the orientation of the correlation field. The large area of the WIR ($4.61 \times 10^5\,km^2$) is presumed to be the result of offshore transport of sediment during the northeast wind regime, or as discussed below, partially the result of organic detritus from phytoplankton blooms stimulated by resuspension of benthic nutrients.

In spite of the fact that annual cumulative discharge was very different in the years we considered (1998–2000), the seasonal patterns for each of the years studied were similar to those shown for 1999. (Rough comparisons can be made by viewing the avi file that accompanies this issue.) For example, all correlation fields generated for the January–March period show smaller DIRs that trend toward the southwest and originate near South Pass. During the April–June period in 1998 and 1999 (and to a lesser extent in 2000), the DIR was close to the coast and extended a considerable distance to the west. In addition, the occurrence of DIRs primarily to the east of the Mississippi occurred only during the July through September season of all 3 years.

5. Discussion

The influences of wind and discharge on suspended particle concentrations in the northern Gulf of Mexico were investigated using a simple correlation approach. We identified two distinct suspended particle provinces (DIRs and WIRs). In the DIRs, time-varying SPM was significantly correlated to the discharge of the Mississippi and Atchafalaya rivers. The particles in these surface waters may be sediments carried by the river plumes, or they may be organic detritus created by phytoplankton that have been stimulated by riverine nutrient fluxes. The SPM algorithm used in this study responds to particles that backscatter light at 670 nm, and thus does not differentiate between sediment and detritus. In the WIRs, SPM is significantly correlated to local wind stress. We infer that the WIRs are influenced by wind-driven resuspension and subsequent transport processes.

These two regions, each with relatively high sediment concentrations, could not be distinguished in conventional satellite-derived sediment maps such as Fig. 2. We have demonstrated that it is possible to distinguish the two regions by their covariance with the dominant processes affecting the suspended particle concentration. Using these methods, investigators interested in ecosystems dominated by one process or the other can confine the focus of their work.

An unexpected finding was the degree to which the DIRs and WIRs were spatially disjointed. This suggests the independence of the two particle-influencing processes and demonstrates the lack of correlation between the discharge and wind data. The wind field in the northern Gulf of Mexico and the Mississippi discharge vary on different temporal scales. Typically, variability in both the direction and intensity of the wind is dominated by the passage of seasonal cold fronts, that occur with a frequency of 3–7 days (Chuang and Wiseman, 1983). Mississippi discharge varies on an annual

cycle with subannual variability dependent on the distribution of precipitation over the drainage basin and differential routing characteristics.

The seasonal variability in the spatial orientation and extent of the DIR was another important finding. Considering all analyses, the distal extent of the DIRs had a spatial range of over 800 km, indicating that the Mississippi can influence vast regions of the Gulf of Mexico. In the spring months, the DIR extended quite far (~400 km) along the Lousiana-Texas coast while in the summer seasons, it was located offshore and to the southeast of the river mouth.

Several studies have documented the presence of Mississippi water and associated particles on the Louisiana-Texas Shelf during the spring season. Dinnel and Wiseman (1986) deduced that much of the annual flux of freshwater to the Louisiana-Texas Shelf, which is highest in the spring, originates from the Mississippi System. Li et al., 1997 used data compiled from 25 cruises (over hydrographic 2000 stations) to document the mean seasonal salinity fields on the Louisiana-Texas Shelf. During the spring, average salinity contours were close to the coast and narrowly spaced showing a strong gradient. These authors pointed out that the along-shelf component of wind stress that generally occurs each spring is expected to force onshore surface Ekman transport which results in a down coast geostrophic flow of Mississippi-Atchafalaya water over the shallow Louisiana-Texas Shelf. Sahl et al. (1997) found that near-surface particle distributions were similar to salinity patterns based on measurements taken in April–May 1993. These authors reported a turbid, low-salinity surface layer associated with the Mississippi extending across much of the Louisiana-Texas Shelf.

The large offshore extent of the DIR in the summer months (July–September) is notable. Although there is ample evidence that the Mississippi discharge mixes with the clearer offshore waters (Morey et al., 2003; DelCastillo et al., 2001; Müller-Karger, 2000; Müller-Karger et al., 1991), and at times even exits the Gulf of Mexico (Atkinson and Wallace, 1975), we caution that the DIR is not necessarily an expression of particle-laden Mississippi River water. There are several reasons for this. In the first place, a high correlation between SPM and discharge does not imply high SPM concentrations, only that the time-varying signals are in phase. Secondly, we are not convinced such a large correlation field is fully attributable to the backscattering of particles originating from the Mississippi. Correlation at the distal reaches of the field may be partially the result of detrital backscatter associated with phytoplankton growth stimulated by nutrient-rich Mississippi water.

Regions identified as discharge influenced were sometimes found in waters where river-borne sediments are normally not found. We attempted to eliminate spurious high correlations offshore by masking pixels with low temporal variances, but there remained high correlations in waters far removed from the mouths of the Mississippi and Atchafalaya rivers. Upon closer inspection, we found that the SPM and chlorophyll values, both derived from SeaWiFS data, covaried in these offshore waters, whereas in areas closer to shore, there was no significant correlation between the satellite chlorophyll value and the SPM calculated by our algorithm. We suggest that in turbid waters the biological and sedimentological processes are uncoupled, but in clearer waters the covariance analysis is affected by biological processes. Nutrients carried in the Mississippi plume enhance productivity, particularly at the euphotic, distal reaches of the plume (Lohrenz et al., 1999). Abundant detrital by-products found within eutrophic waters can increase the backscatter at 670 nm, and thus affect the SPM algorithm results (Mark Dowell, pers. comm, 2002). Furthermore, if chlorophyll levels are high enough, the solar-stimulated fluorescence of chlorophyll *a* at 685 nm would also affect the SPM algorithm in eutrophic waters. The enhanced production is *affected by* the river discharge, and even though the signal may not be accurately interpreted as riverine SPM, the waters are nevertheless influenced by the Mississippi River System as indicated by their covariance with its discharge.

Although the seasonal correlation analyses were carried out with coincident time series (no lag), the correlation between discharge and SPM concentrations in the offshore regions would be expected

to have a higher correlation if the latter were lagged by several days. We performed several correlation analyses in which the SPM time series lagged the discharge. Lag analyses showed maximum correlations at ~10–15 days in the offshore region. River waters transported this distance would require a $\sim 30\,cm\,s^{-1}$ current, which is reasonable in the presence of a warm core eddy. Current speeds in excess of 4 knots ($\sim 200\,m\,s^{-1}$) have been reported in such eddies.

For this study, the surface area of the seasonal DIR was apparently not a function of discharge, and indeed the largest DIR was associated with a low to modest discharge regime. In this respect, our study corroborates the finding of Walker (1996) that the Mississippi River plume responds differently to winds under varying conditions of buoyant stability. Although we had no knowledge of the actual status of buoyant stability, riverine discharge and high sea surface temperatures suggest stratified conditions. If these conditions are accompanied by light winds that do not break down the stratification, the plume can spread with little resistance (Kudryavtsev and Soloviev, 1989).

6. Conclusions

In most cases, the seasonal variability in the orientation and spatial extent of the DIR could be explained by a combination of wind stress, direction, and Ekman dynamics. The alongshore component of the geostrophic wind appears to be largely responsible for the orientation of the plume during most seasons, and Ekman transport (movement to the right of the wind vector) is usually apparent. The effects of tides, Coriolis acceleration, or the presence of eddy structures were not directly considered as forcing functions for this study.

WIRs were generally constrained to shallow waters with the seaward extent of the largest nearly reaching the 100 m contour. We believe WIRs are initially formed by wind generated resuspension processes that occur only in shallow waters, and as such, there was less spatial variability displayed by the WIRs compared to the DIRs. WIRs tended to be smaller when average winds were light and largest when they were strong (Table 2). The two largest WIRs occurred during the months of October through December (1999 and 2000) when the stress-weighted wind was predominately from the northeast. We infer that northeast winds during these seasons aided the offshore transport of sediment, thus increasing the spatial extent of the WIRs.

We believe the methods contained in this work represent important progress toward understanding the spatio-temporal distribution of particles influenced by distinct forcing mechanisms. Further, our findings represent a step toward the independent tracking and understanding of transformation and fate of riverine and wind-influenced constituents. However, future work in this area should include rigorous validation efforts to determine the distribution of the particle fields and their forcing mechanisms in both time and space. Algorithms used to retrieve particle concentrations need to be improved and discrimination between organic and inorganic particles remains problematic using the present generation of algorithms. Much work is also required to resolve vertical particle distributions and to determine the relationship, if any, between surface concentrations and the particle mass within the water column.

7. Video loop

On the compact disk that accompanies this issue, we have provided a video loop entitled "Covariance of Mississippi discharge and satellite-derived sediment estimates January 1, 1998–December 2000". This loop demonstrates the behavior of the DIR and its response to wind stress over time. To make the loop we ran individual 70-day correlation analyses for the entire time period indicated, making individual images of each analysis. A total of 1055 images were composited to create the loop and each was filtered using a 5×5 median filter. The date of the beginning of the individual correlation runs is printed in the upper right of each image. To the right are wind rose histograms corresponding to the 70 days of data used in the correlation analyses. Each

directional count has been weighted by the wind stress value to emphasize the directional components from which the wind is most intense. (See text for details)

The video loop highlights several of the points made in the paper and demonstrates the considerable spatial variability in the DIR as it moves through time. Unlike analyses documented in the text that used a search algorithm to select significantly correlated pixels proximal to the Mississippi outfall, all pixels significantly correlated with Mississippi discharge in the northern Gulf of Mexico are represented. Also, no variance mask was used on these data. Larger rivers whose discharge covaries with the Mississippi are likely to express a correlation structure near the river mouth. Such structures can be seen at the mouths of the Alabama, Suwannee and Sabine Rivers. Interesting excursions of the DIR to the south and east can be seen in late summer, early fall for 1998, 1999 and to lesser extent 2000. Although the trajectory of the DIR can be partially explained by the wind field, this region was under the influence of anticyclonic circulation set up by warm core incursions (DelCastillo et al., 2001; Müller-Karger, 2000).

Acknowledgements

We deeply appreciate the help and professional efforts of Stanley Glidden, Alex Proussevitch and Timothy Moore. Insightful critique, advice and information were generously given by Mark Dowell, Jaime Pringle, Michele Meybeck, Doug Vandemark and Carlos DelCastillo. We gratefully acknowledge the support given by the NASA Biological Oceanography and Land Surface Hydrology Programs. Grants # NAG5-6452 and NAG5-10260.

References

Adams, C.E., Wells, J.T., Coleman, J.M., 1982. Sediment transport on the central Louisiana continental shelf. Implications for the developing Atchafalaya River Delta. Contributions to Marine Science 25, 133–148.

Allison, M.A., Kineke, G.C., Gordon, E.S., Goñi, M.A., 2000. Development and reworking of an annual flood deposit on the inner continental shelf off the Atchafalaya River. Continental Shelf Research 20, 2267–2294.

Amon, R.M.W., Benner, R., 1996. Photochemical and microbial consumption of dissolved organic carbon and oxygen in the Amazon River system. Geochemica et Cosmochemica Acta 60 (10), 1783–1792.

Atkinson, L.P., Wallace, D., 1975. The source of unusually low surface salinities in the Gulf Stream off Georgia. Deep-Sea Research 22 (12), 913–916.

Baith, K., Fu, G., McClain, C.R., 2001. SeaDAS: data analysis system developed for Ocean Color Satellite sensors. EOS Transactions of American Geophysical Union 82, 202.

Booth, J.G., Miller, R.L., McKee, B.A., Leathers, R.A., 2000. Wind-induced bottom sediment resuspension in a microtidal environment. Continental Shelf Research 20 (7), 785–806.

Chen, X., Lohrenz, S.E., Wiesenburg, D.A., 2000. Distribution and controlling mechanisms of primary production on the Louisiana-Texas continental shelf. Journal of Marine Systems 25 (2), 179–207.

Chuang, W.S., Wiseman, W.J., 1983. Coastal Sea-Level response to frontal passages on the Louisana-Texas Shelf. Journal of Geophysical Research 88 (NC4), 2615–2620.

Cloern, J.E., 1987. Turbidity as a control on phytoplankton biomass and productivity in estuaries. Continental Shelf Research 7 (11–12), 1367–1381.

Cochrane, J.D., Kelly, F.J., 1986. Low frequency circulation on the Texas-Louisiana continental shelf. Journal of Geophysical Research 91 (C9), 645–659.

DelCastillo, C.E., Conmy, R.N., Muller-Karger, F.E., Vanderbloemen, L., Vargo, G.A., 2001. Multispectral in situ measurements of organic matter and chlorophyll fluorescence in seawater: documenting the intrusion of the Mississippi River Plume on the West Florida Shelf. Limnology and Oceanography 46 (7), 1836–1843.

Demaster, D.J., Smith, W.O.J., Nelson, D.M., Aller, J.Y., 1996. Biogeochemical processes in Amazon shelf waters: chemical distributions and uptake rates of silicon, carbon and nitrogen. Continental Shelf Research 16 (5–6), 617–628.

Dinnel, S.P., Wiseman, W.J., 1986. Freshwater on the Louisiana and Texas Shelf. Continental Shelf Research 6 (6), 765–784.

Drake, D.E., Cacchione, D.A., 1986. Field observations of bed shear stress and sediment resuspension on continental shelves, Alaska and California. Continental Shelf Research 6 (3), 415–429.

Fekete, B.M., Vorosmarty, C.J., Grabs, W., 1999. GRDC Report Number 22: Global composite runoff fields based on observed river discharge and simulated water balances. Global Runoff Data Center, Koblenz, Germany.

Fong, D.A., Geyer, W.R., 2001. Response of a river plume during an upwelling favorable wind event. Journal of Geophysical Research 106 (C1), 1067–1084.

Fong, D.A., Geyer, W.R., 2002. The alongshore transport of freshwater in a surface-trapped river plume. Journal of Physical Oceanography 32, 957–972.

Garvine, R.W., 1995. A dynamical system for classifying buoyant coastal discharges. Continental Shelf Research 15, 1585–1596.

Goolsby, D.A., Battaglin, W.A., 2001. Long-term changes in concentrations and flux of nitrogen in the Mississippi River Basin. Hydrological Processes 15 (7), 1209–1226.

Gutierrez de Velasco, G., Winant, C.D., 1996. Seasonal patterns of wind stress and wind stress curl over the Gulf of Mexico. Journal of Geophysical Research 101, 18127–18140.

Hitchcock, G.L., Wiseman, W.J., Boicourt, W.C., Mariano, A.J., Walker, N., Nelsen, T.A., Ryan, E., 1997. Property fields in an effluent plume of the Mississippi River. Journal of Marine Systems 12 (1–4), 109–126.

IOCCG Report Number 3, 2000. Remote sensing of ocean colour in coastal and other optically complex waters. In: Sathyendranath, S. (Ed.) International Ocean Color Coordinating Group (IOCCG), Dartmouth, Nova Scotia, Canada.

Justic, D., Rabalais, N.N., Turner, R.E., Dortch, Q., 1995. Changes in the nutrient structure of river dominated coastal waters–stoichiometric nutrient balance and its consequences. Estuarine Coastal and Shelf Science 40 (3), 339–356.

Justic, D., Rabalais, N.N., Turner, R.E., 2002. Modeling the impacts of decadal changes in riverine nutrient fluxes on coastal eutrophication near the Mississippi Delta. Ecological Modelling 152 (1), 33–46.

Kirk, J.T.O., 1994. Light and Photosynthesis in Aquatic Ecosystems. Cambridge University Press, Cambridge 470pp.

Kudryavtsev, V.N., Soloviev, A.V., 1989. Slippery near-surface layer of the ocean arising from daytime solar heating. Journal of Physical Oceanography 20, 617–628.

Large, W.G., Pond, S., 1981. Open ocean momentum measurements in moderate to strong winds. Journal of Physical Oceanography 11, 324–336.

Li, Y., Nowlin, W.D., Ried, R.O., 1997. Mean Hydrographic fields and interannual variability over the Texas-Louisiana continental shelf in spring. Journal of Geophysical Research 102 (C1), 1027–1049.

Lohrenz, S.E., Fahnenstiel, G.L., Redalje, D.G., Lang, G.A., Dagg, M.J., Whitledge, T.E., Dortch, Q., 1999. Nutrients, irradiance, and mixing as factors regulating primary production in coastal waters impacted by the Mississippi River plume. Continental Shelf Research 19 (9), 1113–1141.

Long, E.R., 2000. Environmental Monitoring and Assessment 64 (1), 391–407.

McClain, C.R., et al., 2000. SeaWiFS postlaunch calibration and validation analyses, Part 2. In: Hooker, S.B., Firestone, E.R. (Eds.), NASA Technical Memo 2000-206892. 10, NASA Goddard Flight Center.

McKee, B.A., Aller, R.C., Allison, M.A., Bianchi, T.S., Kineke, G.C., 2004. Transport and transformations of dissolved and particulate materials on continental margins influenced by major rivers: benthic boundary layer and seabed processes. Continental Shelf Research 24 (7–8), 899–926.

Mertes, L.A.K., Warrick, J.A., 2001. Measuring flood output from 110 coastal watersheds in California with field measurements and SeaWiFS. Geology 29 (7), 659–662.

Meybeck, M., 1982. Carbon, nitrogen and phosphorous transport by world rivers. American Journal of Science 282, 401–450.

Milliman, J.D., Meade, R.H., 1983. World -wide delivery of sediment to the world's oceans. Journal of Geology 91, 1–21.

Moeller, C., Gunshor, M.M., Menzel, W.P., Huh, O.K., Walker, N.D., Rouse, L.J., 2001. Recent monitoring of suspended sediment patterns along Louisiana's coastal zone using ER-2 based MAS data and TERRA based MODIS data. 11th Conference on Satellite Meteorology and Oceanography, Madison, WI, 15–18 October 2001 (preprints). Boston, MA, American Meteorological Society, pp. 65–68.

Morey, S.L., Schroeder, W.W., O'Brien, J.J., Zavala-Hidalgo, J., 2003. The annual cycle of riverine influence in the eastern Gulf of Mexico. Geophysical Research Letters 30 (16), 1867–1871.

Müller-Karger, F.E., McClain, C.R., Fisher, T.R., Esaias, W.E., 1989. Pigment distributions in the Carribbean Sea: observations from space. Progress in Oceanography 23, 23–64.

Müller-Karger, F.E., 2000. The Spring 1998 NEGOM Cold Water Event: remote sensing evidence for upwelling and for eastward advection of Mississippi Water (or: How an Errant LC Anticyclone Took the NEGOM for a Spin). Gulf of Mexico Science 1, 55–67.

Müller-Karger, F.E., Walsh, J.J., Evans, R.H., Meyers, M.B., 1991. On the seasonal phytoplankton concentration and sea surface temperature cycles of the Gulf of Mexico as determined by satellites. Journal of Geophysical Research 96 (C7), 12645–12665.

Murray, S.P., 1972. Observations on wind, tidal and density driven currents in the vicinity of the Mississippi River Delta. Shelf Sediment Transport. In: Swift, Duane, Pilkey (Eds.), DH&R Stroudsburg, PA, pp. 127–142.

Myint, S.W., Walker, N.D., 2002. Quantification of surface suspended sediments along a river dominated coast with NOAA AVHRR and SeaWiFS measurements, Louisina, USA. International Journal of Remote Sensing 23 (16), 3229–3249.

NASQAN, 2002. USGS National Stream Quality Accounting Network. Sediment data for Mississippi River. URL: http://water.usgs.gov/nasqan/.

NSF, 2002. National Fisheries Service Statistics. Personal communication from the National Marine Fisheries Service, Fisheries Statistics and Economics Division, Silver Spring, MD.

O'Reilly, J.E., et al., 2000. Ocean Chlorophyll a algorithms for SeaWiFS OC-2 and O-4, Version 4. In: Hooker, S.B., Firestone, E.R. (Eds.), Part 3. NASA Technical Memo 2000–206892. 10, NASA Goddard Flight Center.

Ortner, P.B., Hill, L.C., Cummings, S.R., 1989. Zooplankton community structure and copepod species composition in

the northern Gulf of Mexico. Continental Shelf Research 9 (4), 387–402.

Rabalais, N.N., Wiseman, W.J., Turner, R.E., SenGupta, B.K., Dortch, Q., 1996. Nutrient changes in the Mississippi River and system responses on the adjacent continental shelf. Estuaries 19 (2B), 386–407.

Rouse, L.J., Coleman, J.M., 1976. Circulation observations in the Louisiana Bight using LANDSAT imagery. Remote Sensing of Environment 5, 55–66.

Sahl, L.E., Wiesenburg, D.A., Merrell, W.J., 1997. Interactions of mesoscale features with Texas shelf and slope waters. Continental Shelf Research 17 (2), 117–136.

Salisbury, J.E., Campbell, J.W., Meeker, L.D., Vorosmarty, C.J., 2001. Ocean color and river data reveal fluvial influence in coastal waters. EOS Transactions, American Geophysical Union 82:20 (221), 226–227.

Siddorn, J.R., Bowers, D.G., Hoguane, A.M., 2001. Detecting the Zambezi River Plume using observed optical properties. Marine Pollution Bulletin 42 (10), 942–950.

Siegel, H., Gerth, M., 2000. Satellite-based studies of the 1997 Oder flood event in the southern Baltic Sea. Remote Sensing of Environment 73, 207–217.

Siegel, D.A., Wang, M.H., Maritorena, S., Robinson, W., 2000. Atmospheric correction of satellite ocean color imagery: the black pixel assumption. Applied Optics 39 (21), 3582–3591.

Stumpf, R.P., 1988. Sediment transport in Chesapeake Bay during floods. Analysis using satellite and surface observations. Journal of Coastal Research 4 (1), 1–15.

Stumpf, R.P., Goldschmidt, P.M., 1992. Remote sensing of suspended sediment discharge into the western Gulf of Maine during the 1987 100-year flood. Journal of Coastal Research 8 (1), 218–225.

Stumpf, R.P., Pennock, J.R., 1989. Calibration of a general optical equation for remote sensing of suspended sediments in a moderately turbid estuary. Journal of Geophysical Research 94 (C10), 14363–14371.

Stumpf, R.P., Gelfenbaum, G., Pennock, J.R., 1993. Wind and tidal forcing of a buoyant plume, Mobile-Bay, Alabama. Continental Shelf Research 13 (11), 1281–1301.

Tassan, S., Sturm, B., 1986. An algorithm for the retrieval of sediment content in turbid coastal waters from CZCS data. International Journal of Remote Sensing 7 (5), 643–655.

Turner, R.E., Qureshi, N., Rabalais, N.N., Dortch, Q., Justic, D., Shaw, R.F., Cope, J., 1998. Fluctuating silicate: nitrate ratios and coastal plankton food webs. Proceedings of the National Academy of Sciences of the United States 95 (22), 13048–13051.

Villaescusa-Celaya, J.A., Gutierrez-Galindo, E.A., Flores-Munoz, G., 2000. Heavy metals in the fine fraction of coastal sediments from Baja California (Mexico) and California (USA). Environmental Pollution 108 (3), 453–462.

Walker, N.D., 1996. Satellite assessment of Mississippi Plume variability: causes and predictability. Remote Sensing of Environment 58, 21–35.

Walker, N.D., Hammack, A.B., 2000. Impacts of winter storms on circulation and sediment transport, Atchafalaya-Vermillion Bay region, Louisiana, USA. Journal of Coastal Research 16 (4), 996–1010.

Walker, N.D., Fargion, D., Rouse, L.J., Biggs, D., 1994. Circulation of the Mississippi River water discharged into the northern Gulf of Mexico by the Great Flood of 1993. EOS Transactions, American Geophysical Union 75:35 (409), 414–415.

Whitlock, C.H., Poole, L.R., Usry, J.W., Houghton, W.M., Witte, W.G., Morris, W.D., Gurganus, E.A., 1981. Comparison of reflectance with backscatter and absorption parameters for turbid waters. Applied Optics 20 (3), 517–522.